



Analysis) program package, incorporating several main programs and a set of pre- and post-processors. The procedure of computations, as it has been applied so far, encompasses three successive stages (Fig. 2).

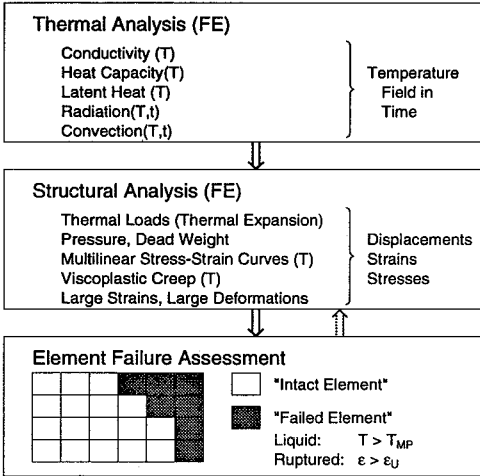


Figure 2: Computational strategy.

In the first stage, a thermal analysis is carried out, with different thermal boundary conditions which simulate the thermal attack on the crucible bottom in various ways. The code ADINA-T allows for all kinds of boundary conditions as well as for arbitrary temperature dependence of the material constitutive properties. So far we consider only material behaviour for solids. In the thermal analysis, only the original geometry of the structure can be considered; thus deformations which, for instance, result from the thermal expansion or from the melting material, are not taken into account.

In the second stage, a stress analysis is performed assuming the thermally induced loads computed before, but without any further interactions with the thermal analysis. Both dead weight and pressure can be applied as mechanical loads. ADINA allows arbitrary, nonlinear stress-strain relations, ranging from elastic to fully plastic behaviour, with temperature dependence.

In the third stage, the solution found in step increments of time must be checked to verify whether in the crucible local or global failure occurs, through a hole or by tearing off of the whole bottom plate. For this obvious check, special termination criteria (resp. the melting point  $T_{MP}$  and the ultimate strain  $\epsilon_U$ ) must be used within the computer code, to establish from which conditions onwards the character of the problem is fundamentally changed, e.g. by melt outflow.

## 2 COMPUTATIONAL METHODS

### 2.1 Thermal analysis

The thermal analysis of the crucible bases on a FE temperature field calculation which uses solid material conduction elements. In general the discretisation (Fig. 3) was made according to the expected temperature gradients. Towards the contact surface of melt and structure smaller size elements were chosen. The model was di-

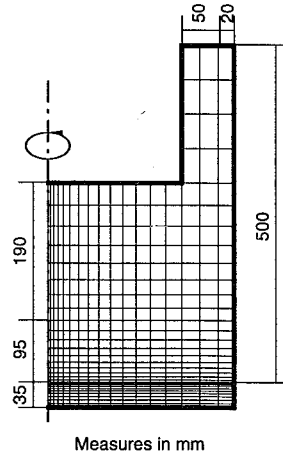
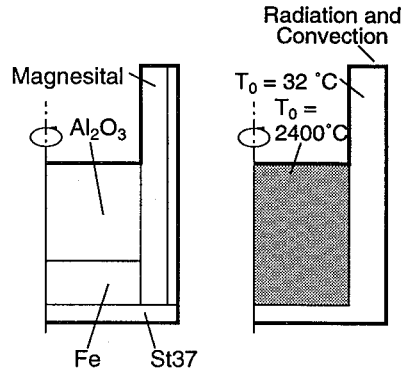


Figure 3: Temperature field model with boundary and initial conditions

vided into 5 element groups according to the different materials in the experimental setup [1]. The final FE mesh had 538 nodes.

Standard Gauss integration was used, and the Euler-backward time integration was applied.

Initial condition was room temperature (32 °C) for the crucible, and 2400 °C for the melt. We considered latent heat at the phase changes. This called for use of the lumped form of the conductivity matrix, since

ADINA-T only incorporates latent heat in the lumped form of the conductivity matrix. The accuracy of the solution is influenced in the lumped form at the rotational symmetry axis, therefore the mesh was refined towards it. Further we considered free convection and radiation at all the free surfaces. To this end the model encompasses special boundary condition elements. For the free convection a constant value of  $50 \text{ W/m}^2$  was chosen, which is about the maximum heat loss to air by free convection. The radiation elements use the Stefan-Boltzmann law with a temperature dependent emissivity (Fig. 4).

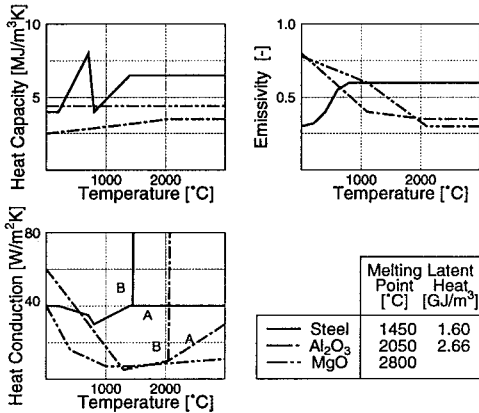


Figure 4: Material parameters

Since the temperature front calculation can only consider conduction in solid structures, an engineering approach was chosen to simulate the heat transfer by convection, leading to two extreme cases. The first 'coldest' condition (model A) considered a steady heat flow with no movement in the melt. The material properties from the higher temperature regions were also used for the solid element formulation. The second 'hottest' model B considered a strong convection. This was simulated by prescribing a very high conduction above the melting point. The value was multiplied by a factor 500. Parameter studies showed no sensitivity to this factor. By doing so two bounding models were obtained.

Extensive material parameter studies were performed, the choice of the material parameters (Fig. 4) within the spread of the material parameter band is based on conservative assumptions. Conservative in this connection means: the greatest thermal load on the structure, to be sure that if even under these assumptions no failure is calculated, it will definitely not occur in practice.

In the calculation special care is required of the temperature and stress fields due to the shock-like thermal loading. The high temperature gradients easily lead to numerical difficulties or inaccuracies.

CPU time varied from 80 sec for a coarse mesh with 28 time steps to 220 sec for the finest version, calculated on a CRAY-2 computer. Models used as input for the structure mechanics calculation needed about 150 sec at 67 timesteps on a HP-730 workstation.

## 2.2 Structural analysis

The presented analysis is still in research, and the given results can therefore only be considered qualitatively. One of the main problems in developing the computational model is the low level of today's state of the art in the field of thermomechanics in the high temperature range of solid metals. The reasons for these difficulties are that material behaviour and thus the incorporated material laws are complex and that the required material properties for temperatures in excess of  $600 \text{ }^\circ\text{C}$  are difficult to determine and therefore scarce in the published literature.

The structural analysis uses a separate temperature input as load. A set of temperature dependent bilinear stress-strain curves are used as material model. Special 9 node elements were used, with 3 pressure trial functions per element. Standard 3x3 Gauss integration was applied. For time integration the 'Full-Newton' method with line search was used.

The strong temperature jump applied in the temperature field calculations caused major problems in stability when applying these results in a thermoplastic structural model. Therefore several adaptations were made. First, to overcome the sudden temperature impact, the initial temperature of  $2400 \text{ }^\circ\text{C}$  was applied in a few time steps, before letting the system transport the input heat. Secondly, the temperature jump on the edge of the attacked bottom plate was spread over a few elements, hence simulating leakage in the lower edge of the insulation, and hindering the sudden attack.

Even with these measures, the startup phase of the thermoplastic calculations required a very fine timestep and mesh discretisation. Major mesh refinement was necessary in the corner where the bottom plate is attached to the crucible side wall. The presented FE structural mesh has 3025 nodes.

CPU-requirements can reach up to 30 000 s on a HP-730 workstation for 1200 time steps.

## 2.3 Element failure assessment

To come to a prediction on total structure failure, we first have to decide whether an element in the calculation is still intact or not. This element failure check is performed without feedback to the structural calculation. In a post processing run elements are checked if they have exceeded temperature or strain limits, and are removed graphically from the result plots. In future calculations a method will be studied to eliminate failed elements from the structure within the calculation. With this feedback procedure we hope to come to

a more satisfying description of the behaviour, and to obtain less numerical disturbance.

### 3 RESULTS

#### 3.1 Thermal behaviour

In the temperature field calculations a reasonable agreement was found with experimental results, considering the inaccuracy of the initial and boundary conditions.

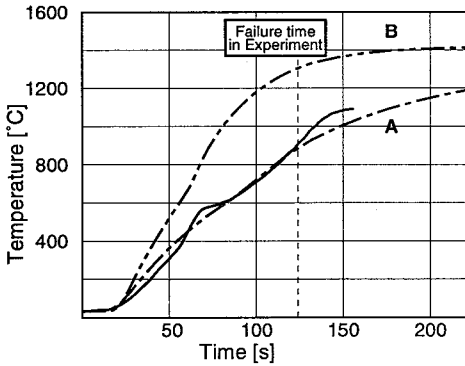
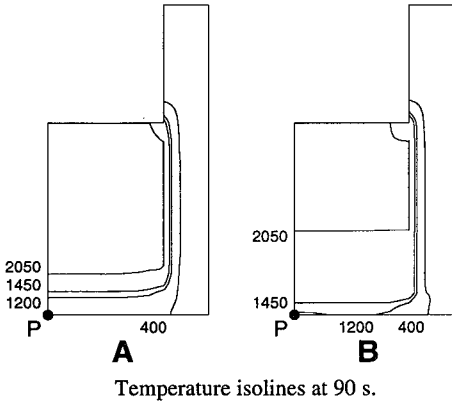


Figure 5: Comparison with experimental temperature measurements at the centre P

Fig. 5 shows the curves for the two above-mentioned extreme boundary conditions (models A and B) compared with the thermocouple measurement of the experiment.

In the calculations the time starting point was chosen at the moment when the crucible is filled with melt at a homogenous temperature of 2400 °C. In the experiment this point is not easy to define precisely. The moment when the measured temperature starts to increase at the considered location was chosen as starting point for the experimental results. To match the calculations with the experiment both calculated time histories

were shifted forward by 12 s, which was estimated to be the unknown time of the thermite burn up. With this adjustment a fair agreement was reached between the curve 'A' and the experiment.

However, it must be noted that the experiment showed that the centre of the plate was not the hottest spot of the bottom surface. We presume that the temperature of the actually hottest point (which was under load from convective heat transfer) would be below, but fairly close to curve 'B' in Fig. 5. For the convective state the model B gives a good description, in an area where less movement was recorded model A shows good agreement.

From Fig. 5 also the times of failure can be read. Failure of the crucible was defined to be the moment of melt outflow. A failure time of 124 s. at a temperature of 1200 °C was recorded in the presented experiment. This shows that failure might occur at temperatures lower than the melting point, due to throughgoing material weakening, even in a low pressure case. In our calculation this is modelled by elements exceeding the set strain limit  $\epsilon_U$ . The 1200 °C isotherm reaches the bottom outer surface after about 90 s. in the high conduction model B. In the low conduction model A this value was reached after about 220 s.

Fig. 6 shows the temperature increase at the bottom surface in model B. It shows that when 'uniform' or no convection occurs, the plate heats up steadily over the whole diameter.

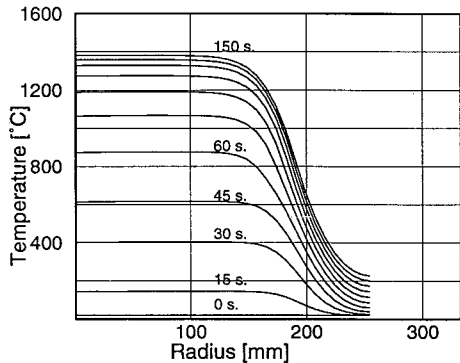


Figure 6: Temperature increase at bottom plate outer surface for model B (high conduction)

#### 3.2 Mechanical behaviour

It is clear that no close comparison in mechanical behaviour with measurements can be made based on temperature fields with an illdefined initial condition. However, a trend in the behaviour can be detected, and this agreed with the phenomenological behaviour of the experimental crucible. Fig. 7 shows the behaviour of the

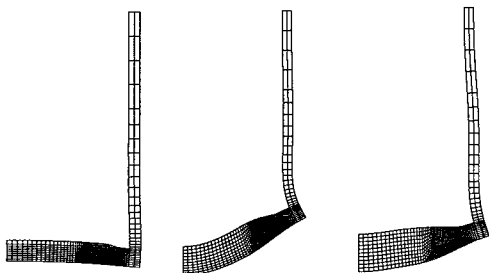


Figure 7: Time history of amplified deformation of heated crucible

heated crucible, after applying a temperature load obtained from the above described model B. The initial temperature introduces thermal strains. Therefore the inner surface expands first, which causes the bottom plate to bend upwards. As the heat front progresses through the plate, the load causes the plate to sag, due to diminishing strength.

The progression of the plastic zone will give an indication of the failure process, in the case of low pressure loading, hence the plastification is due to exceeding the temperature thresholds there where major material weakening occurs.

#### 4 OUTLOOK

The experiment [1] showed a rather violent disturbance in the melt, indicating strong convection. This calls for an improved model using fluid flow elements for the melt. Studies showed great difficulty in adapting FE-fluid mechanics with heat transfer to problems with very high turbulent convective heat transfer. In a later stage this will also be implemented.

The thermal load in the CORVIS experiments causes a different failure mechanism than when a mass of debris is piled upon the structure [2], since the debris are at lower temperature and the thermal contact is not good. The thermal load will spread over a much longer time. In that case it is necessary to consider creep rupture as well. In this case the gradients are smaller, and the numerical stability higher.

Methods to integrate element failure within the structural calculation will be studied. In this way, a feedback is produced to the structural analysis. Special attention is due to transferring pressure load across failed elements.

#### 5 CONCLUSIONS

A RPV failure assessment was presented, based on the FE-method. We propose a stepwise procedure consist-

ing of a thermal analysis, followed by a structural analysis in which the obtained temperature fields are used as load. In a third step a decision is made on failure through special failure criteria.

The FE-method gives a good insight in the temperature field behaviour, if one realises the given restrictions. The temperature advance in a solid can be computed accurately. When violent convection cells develop, there is a need for a fluid flow calculation. The high temperature gradients in the particular CORVIS case presented here will give rise to various numerical problems. To a certain extent it is questionable whether the FE-method is suited for a problem like this. With worked-out adaptations in assessing failure, and eliminating from the calculation failed parts, which would cause numerical disturbance, a fair description of failure mechanisms is possible. In an actual RPV severe accident one will not find these extreme thermal loads, therefore the presented method is suitable for RPV failure research.

#### ACKNOWLEDGEMENTS

We wish to express our gratitude to our colleague K. Reichlin for his support to the present work; To H. Hirschmann, CORVIS project manager and to the members of the experimental team for the realisation of the experiments and the fruitful cooperation. Special thanks are due to Dr. J. P. Hosemann, head of the LWR-Safety program in the Paul Scherrer Institute, who initiated and surveyed the CORVIS project. We gratefully mention the financial assistance from the Swiss Federal Nuclear Safety Inspectorate and from the Swiss Federal Office of Energy.

#### REFERENCES

- [1] Patorski J., Hirschmann H., Peters K. (1993): CORVIS: Investigation of LWR Lower Head Failure Modes, Experimental Programme; Transactions of the 12th SMIRT Conference, Stuttgart.
- [2] Rempe J. et al. (1991): Light Water Reactor Lower Head Failure Analysis NUREG/CR-5642, EGG-2618

